PERGAMON

International Journal of Multiphase Flow 24 (1998) 889–912

International Journal of Multiphase Flow

Temporal properties of secondary drop breakup in the bag breakup regime

W.-H. Chou [1], G.M. Faeth *

Department of Aerospace Engineering, The University of Michigan, Ann Arbor, Michigan 48109-2140, U.S.A.

Received 9 July 1997; received in revised form 1 April 1998

Abstract

The temporal properties of secondary drop breakup in the bag breakup regime were measured as a function of time for shock-wave-initiated disturbances in air at normal temperature and pressure. The test liquids included water, ethyl alcohol and various glycerol mixtures to yield liquid/gas density ratios of 633–893, Weber numbers of 13–20, Ohnesorge numbers of 0.0043–0.0427 and Reynolds numbers of 1550–2150. Single- and double-pulse shadowgraphy and holography were used to measure the structure, size and velocity of the parent drop, and the sizes and velocities of drops produced by secondary breakup. The parent drop undergoes significant deformation and lateral growth during breakup before forming a thin bag having a basal ring that is characteristic of the bag breakup regime. The basal ring contains roughly 56% of the initial drop volume (mass) and eventually yields drops having mean diameters of roughly 30% of the initial drop diameter by a Rayleigh breakup process; the size variations of drops formed from the basal ring increases with increasing Weber number due to the appearance of large 'node' drops that are characteristic of the onset of the multimode breakup regime. Breakup of the bag yields nearly monodisperse drops having diameters of roughly 4% of the initial drop diameter. The velocity distributions of the drops formed from breakup of the basal ring and the bag were individually independent of drop size but varied as a function of time and differed between the two groups. Many features of these phenomena were successfully correlated using phenomenological analyses. Finally, bag breakup requires considerable time (5–6 characteristic secondary drop breakup times) and extends over considerable streamwise distances (50–100 initial drop diameters) by the end of breakup, which suggests that bag breakup should be treated as a rate process, rather than by jump conditions, in some instances.
© 1998 Elsevier Science Ltd. All rights reserved.

Keywords: Drop breakup; Drop dynamics; Pulsed holography; Sprays; Atomization

* Corresponding author.
[1] Currently with the Trane Corporation, LaCrosse, Wisconsin, U.S.A.

0301-9322/98/$19.00 © 1998 Elsevier Science Ltd. All rights reserved.
PII: S0301-9322(98)00015-9

1. Introduction

The secondary breakup of drops is important because primary breakup yields drops that are intrinsically unstable to secondary breakup, while secondary breakup often is the rate controlling process within dense sprays in much the same way that drop vaporization often is the rate controlling process within dilute sprays (Faeth, 1997; Faeth et al., 1995; Wu et al., 1995). Motivated by these observations, the objective of the present investigation was to extend recent studies of the regimes and outcomes of secondary breakup caused by shock-wave disturbances due to Hsiang and Faeth (1992, 1993, 1995), and Chou et al. (1997), to consider the evolution of bag breakup as a function of time.

Several recent reviews of secondary breakup are available, see Faeth (1997), Faeth et al. (1995), Hsiang and Faeth (1992, 1993, 1995), Wu et al. (1995) and references cited therein; therefore, the following discussion of past work will be brief. Shock-wave disturbances were considered during most earlier studies, providing a step change of flow properties around the drop, similar to conditions experienced by drops at the end of primary breakup. Secondary breakup properties that have been considered include the conditions required for particular deformation and breakup regimes, the time required for the onset and end of breakup, the drag properties of deformed drops and the size and velocities of the drops produced by secondary breakup (i.e. the secondary breakup jump conditions). An interesting feature of these results is that secondary breakup extended over appreciable regions of time and space and was not properly described by jump conditions in some instances. For example, Liang et al. (1988) show that breakup times are equal to $5.5t^*$ for a wide range of breakup conditions, where t^* is the characteristic secondary breakup time for shear breakup defined by Ranger and Nicholls (1969) as follows:

$$t^* = d_o(\rho_L/\rho_G)^{1/2}/u_o. \tag{1}$$

In (1) d_o and u_o are the initial drop diameter and relative velocity, ρ denotes density and the subscripts L and G denote liquid and gas properties, respectively. Such times are comparable to flow residence times within the dense spray region where secondary breakup is a dominant process (Faeth, 1997; Faeth et al., 1995; Wu et al., 1995). Viewed another way, the original (or parent) drop moves roughly 50 initial drop diameters, while the smallest drops formed by secondary breakup move up to 100 initial drop diameters, during the period of breakup for typical shear breakup processes (Hsiang and Faeth, 1993, 1995). Such distances can represent a significant fraction of the length of the dense spray region. These observations suggest that the time-resolved features of secondary breakup eventually must be understood, i.e. the size and velocity distributions of the drops, and the rate at which liquid is removed from the parent drop, must be known as a function of time during secondary breakup. Motivated by this observation, the authors and their associates are concentrating on studies of the temporal properties (dynamics) of particular secondary breakup processes.

The first phase of the study of the temporal properties of secondary breakup considered the shear breakup regime where secondary breakup proceeds by the stripping of drop liquid from the periphery of the parent drop (Chou et al., 1997). Other conditions of the shear breakup study included $\rho_L/\rho_G > 680$, where gas-phase processes approximate quasi-steady behavior,

and small Ohnesorge numbers, $Oh = \mu_L/(\rho_L d_o \sigma)^{1/2} < 0.04$, where μ and σ denote viscosity and surface tension, respectively. It was found that the size distributions of drops produced by secondary breakup at each instant of time satisfied the universal root normal distribution function, with $MMD/SMD = 1.2$, due to Simmons (1977), where MMD and SMD denote the mass median and Sauter mean diameters of the drop size distributions, respectively. This behavior is very helpful because this two-parameter distribution function is fully defined by the SMD alone, given the MMD/SMD ratio. In contrast, the velocity distribution functions of drops produced by secondary breakup were uniform. Other measurements of shear breakup properties as a function of time included the size and velocities of the parent drop, the SMD and mean and fluctuating velocities of drops produced by secondary breakup, and the rate of liquid removal from the parent drop due to secondary breakup. All these properties were correlated and interpreted using phenomenological theories, providing the information needed to treat shear breakup as a rate process during computations of spray structure.

The present study seeks to extend information about the temporal properties of secondary breakup from the shear breakup regime to the bag breakup regime. Within the bag breakup regime, secondary breakup proceeds by deformation of the center of the drop into a thin balloon-like bag that extends in the downstream direction from a thicker ring-like structure of its base (the basal ring), with both the bag and the basal ring subsequently dividing into drops. An understanding of bag breakup is important for two reasons: (1) the bag breakup regime bounds the region where drops only deform and do not break up, which provides fundamental clues about the mechanism of the onset of secondary breakup, and (2) the complex multimode breakup regime is bounded by the bag- and shear-breakup regimes which clearly must be understood before addressing the important multimode breakup mechanism (Hsiang and Faeth, 1992, 1993, 1995). Similar to the earlier study of shear breakup, the present study emphasized new measurements of the temporal properties of bag breakup and used phenomenological theories to help interpret and correlate the measurements.

The present measurements were carried out using a shock tube facility, with the environment of the test drops during breakup roughly approximating air at normal temperature and pressure (NTP). Single- and double-pulse shadowgraphy and holography were used to find the properties of the parent drop, the size and velocity properties of drops produced by secondary breakup and the rate of liquid removal from the parent drop as a function of time during breakup. Test conditions were limited to relatively large liquid/gas density ratios ($\rho_L/\rho_G > 500$) and relatively small Ohnesorge numbers ($Oh < 0.1$), within the bag breakup regime where the Weber number, $We = \rho_G d_o u_o^2/\sigma$, is in the range 13–35 (Hsiang and Faeth, 1993). As a result, the present test conditions are most representative of bag breakup within sprays near atmospheric pressure. Drop liquids included water, ethyl alcohol and various glycerol mixtures, in order to provide information about effects of drop liquid properties.

The paper begins with a description of experimental methods. Results are then discussed considering the properties of the parent drop, the properties of the basal ring, the properties of drops formed from the bag itself and the overall properties of bag breakup, in turn. The following description of the study is brief, see Chou (1997) for more details and a complete tabulation of data.

2. Experimental methods

2.1. Apparatus and instrumentation

The test apparatus and instrumentation will be described only briefly because it was similar to earlier work (Hsiang and Faeth, 1992, 1993, 1995; Chou et al., 1997). The arrangement consisted of a rectangular shock tube with the driven section open to the atmosphere. The test location was windowed to allow observations of drop breakup. A vibrating capillary tube drop generator, combined with an electrostatic drop selection system, provided a stream of drops at the test location with sufficient spacing between drops to accommodate bag breakup with negligible drop/drop interactions.

Single- and double-pulsed shadowgraphy and holography were used to observe the properties of the parent drop and the size and velocity distribution functions of drops produced by secondary breakup. Laser pulse times were sufficiently short (7 ns) to stop the motion of drops on the film while using a weaker second laser pulse allowed directional ambiguity to be resolved for velocity measurements. The combined holocamera and reconstruction system allowed objects as small as 3 μm to be observed and as small as 5 μm to be measured with 5% accuracy. Results at each condition were summed over at least four realizations, considering 100–200 liquid elements, in order to obtain drop diameter and velocity correlations. Estimated experimental uncertainties (95% confidence) were less than 10% for drop diameters and less than 15% for streamwise drop velocities.

2.2. Test conditions

The test conditions are summarized in Table 1. The liquid properties were obtained from Lange (1952), except for the surface tensions of the glycerol mixtures which were measured in the same manner as Wu et al. (1991). The ranges of the test variables were as follows: $d_o = 0.62$–0.85 mm, $\rho_L/\rho_G = 633$–893, Oh $= 0.0043$–0.0427, $We = 13$–20 and $Re = 1550$–2150, where the Reynolds number, $Re = \rho_G d_o u_o/\mu_G$. The present We test range is narrow but this is consistent with the narrow We range of the bag breakup regime. The Re range of the present

Table 1
Summary of the test conditions for bag breakup†

Liquid‡	d_o (μm)	ρ_L (kg/m^3)	ρ_L/ρ_G (–)	$\mu_L \times 10^4$ (kg/ms)	$\sigma \times 10^3$ (N/m)	$Oh \times 10^3$ (–)	Re (–)
Water	620	997	755	8.94	70.8	4.3	1670–1910
Ethyl alcohol	630	800	633	16.0	24.0	15.0	1830–2080
Glycerol (21%)	650	1050	806	16.0	67.3	7.5	1550–1660
Glycerol (42%)	650	1105	857	35.0	65.4	16.1	1550–1910
Glycerol (63%)	850	1162	893	108.0	64.8	42.7	1850–2150

†With We in the range 13–20 in air initially at 98.8 kPa and 298 ± 2 K in the driven section of the shock tube. Shock Mach numbers in the range of 1.01–1.04. Properties of air taken for conditions downstream of shock wave: with pressures of 119.7–129.8 kPa, ρ_G of 1.25–1.31 kg/m^3 and μ_G of 18.5×10^6 kg/ms.

‡Glycerol compositions given in parentheses are percent glycerin (by mass) in water.

experiments is higher than conditions where gas viscosity has a significant effect on drop drag properties, e.g. the drag coefficient, C_D, for spheres only varies in the range 0.4–0.5 for this Reynolds number range (White, 1974). Shock Mach numbers were relatively low, less than 1.04; therefore, the physical properties of the gas in the uniform flow region behind the shock wave were nearly the same as room air.

3. Results and discussion

3.1. Parent drop properties

3.1.1. Parent drop size

Fig. 1 is a composite illustration of several aspects of the temporal evolution of bag breakup. The illustration includes: measurements of the parent drop cross-stream diameter d_p, as a

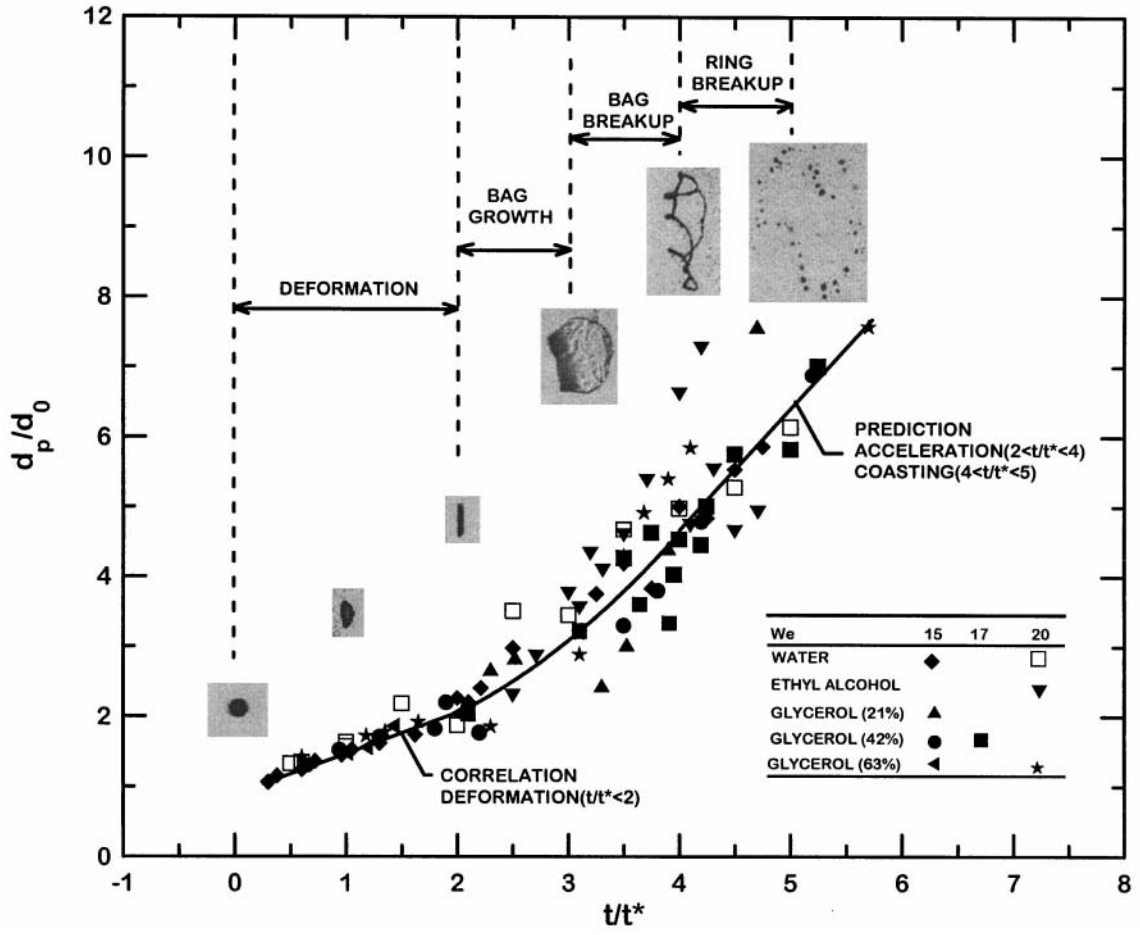

Fig. 1. Parent drop characteristic diameter as a function of time during bag breakup. Note that the shock wave has passed from left to right in the inset photographs.

function of time, t, for water, ethyl alcohol and glycerol drops having We of 13–20 and $Oh \leqslant 0.043$; delineation of the time periods of various portions of the bag breakup process; and inset photographs of the appearance of the parent drop at various times during breakup. The photographs are for a water drop in air subjected to a shock wave disturbance with $We = 20$ and $Oh = 0.0044$. Note that the shock wave passes from left to right in the inset photographs. The various positions of the bag breakup process are defined as follows: the deformation period where the drop deforms from a spherical to a disk-like shape for t/t^* of 0–2; the bag growth period where the center of the disk deforms into a thin membrane-like bag with a much thicker basal ring surrounding its open (upstream) end for t/t^* of 2–3; the bag breakup period where the bag progressively breaks up from its closed downstream end toward the basal ring for t/t^* of 3–4; and the ring breakup period where a series of relatively large node drops form along the ring followed by breakup of the ring into a circular array of relatively large drops to end the breakup process for t/t^* of 4–5. Note that the bag growth and ring breakup periods include a temporal range that is dominated by these processes. The actual time periods when bag and ring breakup occurs are contained in these periods, respectively, but are much shorter. The value of d_p is taken to be the cross-stream diameter of the disk before the basal ring forms ($0 \leqslant t/t^* \leqslant 2$) and the outer diameter of the basal ring when it is present ($2 \leqslant t/t^* \leqslant 5$).

The transition between a spherical drop and a relatively thin disk aligned normal to the flow direction occurs during the deformation period ($0 \leqslant t/t^* \leqslant 2$) illustrated in Fig. 1. The deformation of the parent drop is caused by increased static pressures near the upstream and downstream stagnation points along the axis of the drop, combined with decreased static pressures near the drop periphery due to increased flow velocities in this region. This pressure distribution tends to squeeze the drop into a thin disk-like shape. A detailed analysis of this process was not undertaken; instead, it was found that the deformation process could be expressed reasonably well according to the following empirical correlation suitable for the present range of test conditions:

$$d_p/d_o = 1.0 + 0.5t/t^*, \quad 0 \leq t/t^* \leq 2. \tag{2}$$

Subsequent consideration of parent drop size parameters will focus on the properties of the basal ring. This interest is motivated by the fact that the size of the basal ring ultimately controls the size of the drops formed by basal ring breakup while these drops tend to dominate the size properties of drops formed by bag breakup because they are the largest drops in the size distribution. In addition, subsequent considerations will show that the basal ring, and thus the drops formed from the basal ring, comprise a major fraction of the original volume of liquid in the parent drop.

The results illustrated in Fig. 1 show that the rate of lateral acceleration of the basal ring diameters is largest in the period where the bag is present, with subsequent lateral acceleration progressively becoming small toward the end of the period where the bag itself breaks up. This behavior suggests that the higher pressure within the bag, caused by stagnation of the gas flow relative to the drop by the bag, is mainly responsible for the outward acceleration of the basal ring, as well as for the growth of the bag. This pressure difference progressively disappears as the breakup of the bag itself proceeds so that the basal ring simply continues to coast outward in the latter stages of the breakup process; this behavior is supported by the relatively constant

outward velocity of the basal ring diameter toward the end of the entire breakup process. These ideas are developed in the following to obtain the predicted variation of d_p/d_o as a function of t/t^* for the period $2 \leqslant t/t^* \leqslant 5$ that is illustrated in Fig. 1.

Analysis of basal ring growth was carried out ignoring acceleration of the parent drop, i.e. it was assumed that the relative velocity of the basal ring with respect to the gas is equal to the initial relative velocity, u_o; the variation of the diameter of the basal ring tube itself, d_r, was also neglected even though later considerations will show that this diameter decreases by almost a factor of two during the time period of interest; and circumferential surface tension forces were ignored due to the relatively large diameter of the basal ring at the start of the ring acceleration process. Other assumptions will be discussed as they are introduced. Considering the radial acceleration of the basal ring tube, conservation of momentum yields:

$$\rho_L(\pi^2 d_p d_r^2/4)\,\mathrm{d}^2(d_p/2)/\mathrm{d}t^2 = C_r(\rho_G u_o^2/2)(\pi d_p d_r) \tag{3}$$

where C_r is an empirical constant, somewhat analogous to a drag coefficient, to account for the fact that the pressure difference across the basal ring is only a fraction of the ideal stagnation pressure increase due to effects of gas motion across the basal ring and the motion of the gas in the bag, particularly as breakup of the bag itself proceeds. In (3) it is also assumed that the aspect ratio of the ring, d_p/d_r is relatively large when approximating the ring volume and cross-sectional area. Adopting d_p/d_o and t/t^* as normalized dependent and independent variables, (3) becomes:

$$\mathrm{d}^2(d_p/d_o)/\mathrm{d}(t/t^*)^2 = (4C_r/\pi)(d_o/d_r), \quad 2 \leq t/t^* \leq 4 \tag{4}$$

where the time interval of concern is the period when the bag (or at least a portion of it) is present and where the right-hand-side of this equation is taken to be a constant under the assumptions of the present approximate analysis. The initial conditions for (4) were chosen to match the value of d_p/d_o at $t/t^* = 2$ from (2) while adjusting the initial outward velocity of the basal ring to best fit the present measurements, as follows:

$$t/t^* = 2: \quad d_p/d_o = 2.0, \quad \mathrm{d}(d_p/d_o)/\mathrm{d}(t/t^*) = 0.8. \tag{5}$$

Finally, integrating (4) subject to the initial conditions of (5) and adjusting the value of the constant on the right-hand side of (4) to best fit the present measurements, yields:

$$d_p/d_o = 0.25(t/t^*)^2 - 0.18(t/t^*) + 1.43, \quad 2 \leq t/t^* \leq 4 \tag{6}$$

which is the form that is plotted in Fig. 1. The result implies $C_r \approx 0.04$ in (3), which is reasonable in view of the residual motions of the gas within the bag (particularly toward the end of bag breakup) and the fact that the relative velocity of the parent drop with respect to the gas is only roughly 70–90% of the initial relative velocity during the period of bag growth and breakup.

Proceeding to the basal ring breakup period, it is assumed that the basal ring, and the drops that are formed by breakup of the basal ring, simply coast outward with a constant radial velocity once the bag, and thus the mechanism for a pressure difference across the basal ring, has disappeared. This behavior agrees with the observed variation of d_p in this time period, and involves neglecting the relatively small drag forces on drop liquid elements in the radial

direction. Finally, the value of d_p/d_o at $t/t^* = 4$ is matched to the results of (6) and the outward coasting velocity in the ring breakup period is reoptimized to best fit the measurements. The final variation of d_p/d_o in the ring breakup period then becomes:

$$d_p/d_o = 1.79(t/t^*) - 2.51, \quad 4 \leq t/t^* \leq 6 \tag{7}$$

which is the form that is plotted in Fig. 1.

Taken together, (2), (6) and (7) provide a reasonable correlation of the measured variations of d_p/d_o as a function of t/t^* in Fig. 1. These results suggest that the flow resistance caused by the bag, and the remaining portions of the bag during its breakup period, are mainly responsible for the cross-stream spread of drops formed by breakup of the parent drop, including the large drops resulting from breakup of the basal ring. Stabilization of this motion by surface tension within the deformation period can be important; after all, this mechanism is responsible for controlling drop deformation and for preventing drop breakup in the deformation regime at *We* smaller than the bag breakup regime. Nevertheless, effects of surface tension on the radial dispersion of liquid during bag breakup appear to be relatively small.

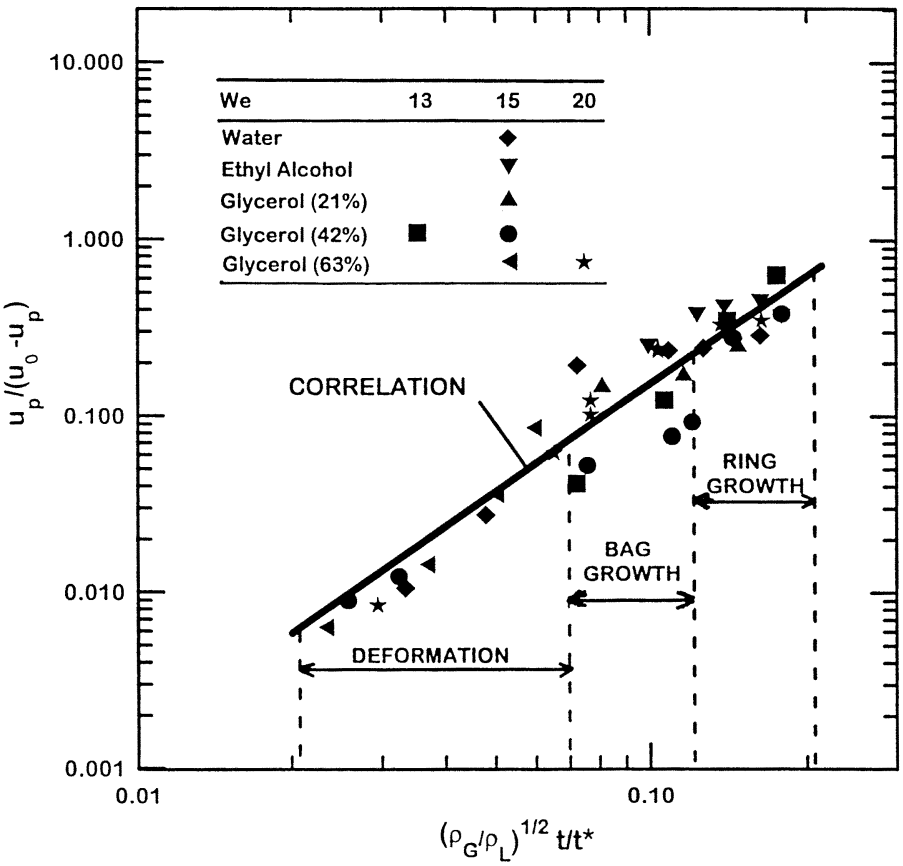

Fig. 2. Parent drop velocity as a function of time during bag breakup.

3.1.2. Parent drop velocities

The velocity of the parent drop, u_p, is plotted as a function of normalized time in Fig. 2. The various breakup periods—deformation, bag growth and basal ring growth (the last combining the bag breakup and ring breakup periods of Fig. 1)—are marked on the plot for reference purposes. The parent drop exhibits considerable acceleration during the breakup period, similar to past observations of the motion of parent drops for shear breakup (Hsiang and Faeth, 1992, 1993, 1995). In fact, the absolute, u_p, and relative, $(u_o–u_p)$, velocities of the parent drop are comparable at the end of the ring growth period, which implies a reduction of the relative velocity of the parent drop of roughly 50% during the time of breakup, which is quite substantial. This behavior comes about due to growth of the cross-stream dimensions of the deformed parent drop, as a result of deformation and bag formation, as well as due to increased drag coefficients of the deformed parent drop, both of which significantly increase the drag forces on the parent drop compared to the original spherical drop.

3.1.3. Drag coefficients

In order to provide a common basis for comparing the drag coefficients of the parent drops during the various breakup periods, they were based on the current (local) cross-sectional area of the drop normal to the flow and relative velocity of the deformed parent drop with respect to the ambient gas. The position of the parent drop was taken to be either the centroid of the deforming drop ($0 \leqslant t/t^* \leqslant 2$) or the axis of the basal ring ($2 \leqslant t/t^* \leqslant 5$). The temporal variation of the temporal drag coefficients are plotted in Fig. 3. The drag coefficients of spheres, $C_D = 0.4$, and thin disks, $C_D = 1.2$, at similar Reynolds numbers are also shown on the plot for reference purposes. In the deformation period ($0 \leqslant t/t^* \leqslant 2$), the drag coefficient increases rapidly as the degree of deformation increases, reaching a maximum value when the bag begins to form. This maximum value approximates the drag coefficient of a thin disk, which is reasonable in view of the shape of the parent drop at this condition. In the bag growth period ($2 \leqslant t/t^* \leqslant 3$), the continuous increase of the cross-stream diameter of the parent drop, along with bag growth (which reduces the transfer of drag forces to the basal ring) causes parent drop drag coefficients to become smaller. The reduced drag of the ring growth and breakup periods ($3 \leqslant t/t^* \leqslant 5$) is then representative of the lost flow resistance of the parent drop once the bag is no longer present.

3.2. Basal ring properties

3.2.1. Basal ring volume

Drop sizes formed from the bag and the basal ring of the bag are substantially different; therefore, it is important to know the relative volumes of the bag and its basal ring in order to estimate drop sizes produced by the bag breakup. Thus, measurements were undertaken to establish the distribution of the parent drop liquid between the bag and the basal ring over the complete range of the present data. These measurements were made by characterizing the ring at the end of bag breakup, including the volume of the nodal drops as well as the cylindrical sections of the ring in the region between the nodal drops. The ratio of the liquid volume in the basal ring, V_r, to the initial volume of the parent drop, V_o, is summarized in Table 2 (other parameters in this table include the Ohnesorge number based on the tube diameter of the ring

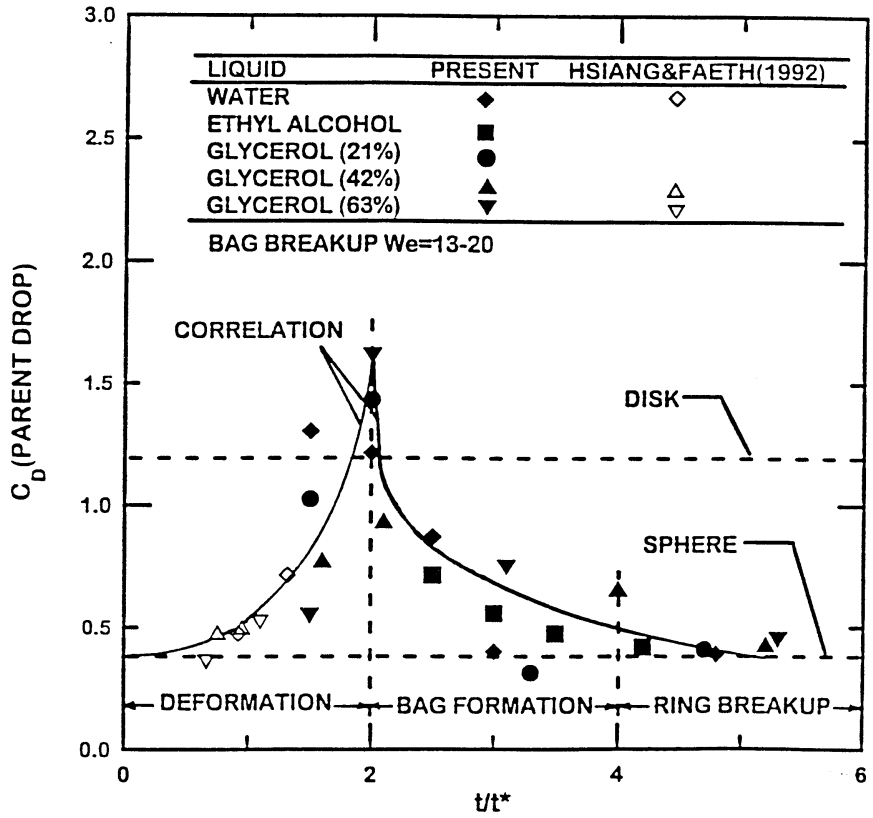

Fig. 3. Parent drop drag coefficient as a function of time during bag breakup.

$Oh_r = \mu_L/(\rho_L d_r \sigma)^{1/2}$, and the diameter of drops formed from the ring, d_{rd}, limited to the properties of the ring between node drops). For present test conditions, each value of Oh corresponds to a particular drop liquid; nevertheless, it can be seen that V_r/V_o is essentially independent of Oh over the present test range, yielding the correlation:

$$V_r/V_o = 0.56 \tag{8}$$

Table 2
Summary of properties of basal ring†

Liquid‡	We	Oh	V_r/V_o	Oh_r	d_{rd}/d_r
Water	15	0.0043	0.57	0.013	2.53
Ethyl Alcohol	15	0.0150	0.52	0.045	2.54
Glycerol (21%)	15	0.0075	0.59	0.021	1.91
Glycerol (42%)	17	0.0161	0.57	0.045	1.87
Glycerol (63%)	15	0.0427	0.54	0.130	2.21

†Result based on the properties of the bag during the bag breakup period for the test conditions summarized in Table 1.

‡Glycerol compositions given in parentheses are percent glycerin (by mass) in water.

with a standard deviation of 0.04. Lane (1951) carried out early measurements of bag breakup and mentions a determination of $V_r/V_o = 0.75$; nevertheless, this earlier value is only mentioned in passing with no information provided about its accuracy and method of determination so that its reliability is uncertain.

3.2.2. Tube axis diameter

Given that the volume of the ring is a fixed fraction of the initial drop volume, it should be possible to determine the diameter of the tube axis of the ring as a function of the ring diameter. In particular, if the presence of node drops along the basal ring is ignored:

$$V_r/V_o = (\pi^2 d_p d_r^2/4)/(\pi d_o^3/6) \tag{9}$$

which implies

$$d_r/d_o = (2V_r/(3\pi V_o))^{1/2}/(d_p/d_o)^{1/2} = 0.35/(d_p/d_o)^{1/2} \tag{10}$$

where d_p/d_o is known as a function of time either from Fig. 1 or from (6) and (7).

Present measurements of d_r/d_o are plotted as a function of t/t^* in Fig. 4. The predictions of d_r/d_o from (10) using (6) and (7) to find d_p/d_o, are also shown on the plot. There is significant

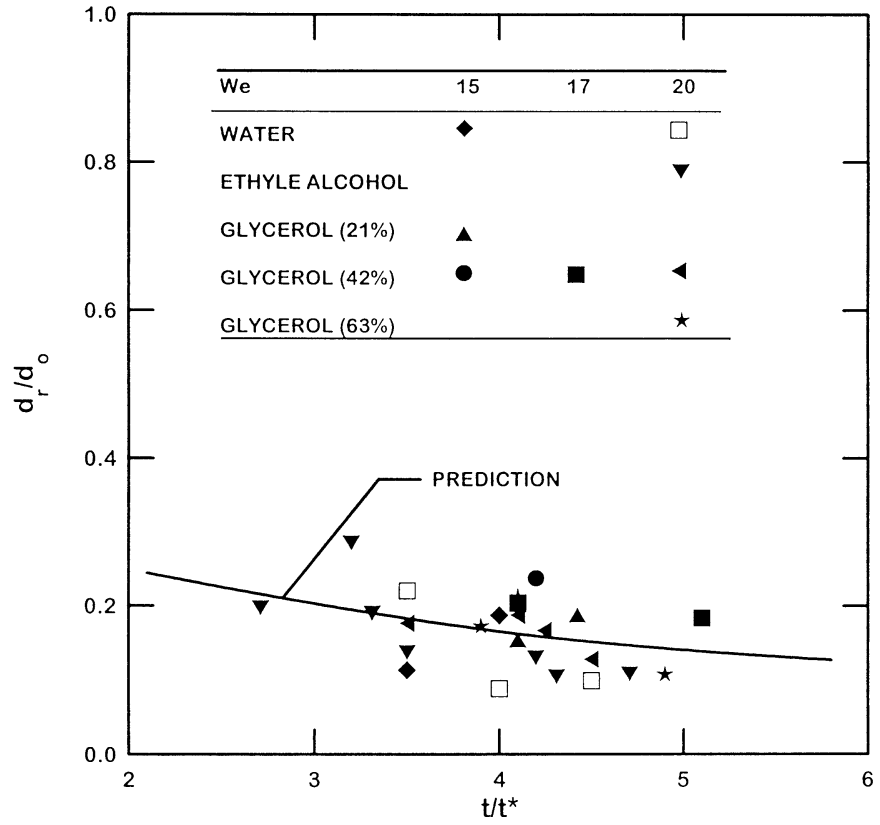

Fig. 4. Ring tube diameter as a function of time during bag breakup.

scatter of the measurements due to problems of observing the basal ring, particularly when the bag is present, and effects of the presence of node drops. Nevertheless, the measurements are in reasonably good agreement with (10), supporting a relatively slow reduction of d_r/d_o with increasing time due to the increased diameter of the tube axis of the basal ring itself.

3.2.3. Basal ring drop diameters

Two types of drops are formed from the basal ring: node drops and drops from the cylindrical portions of the ring between the nodes that are somewhat smaller than the node drops. The drops formed from the cylindrical portion of the basal ring are not subject to strong strain and appear to result from classical Rayleigh breakup of a nearly constant-diameter liquid column. In addition, the Ohnesorge numbers of the rings observed during the present investigation were relatively small ($Oh \leqslant 0.13$ based on values given in Table 2) so that effects of liquid viscosity should be small as well. Under these circumstances, the ratio of the diameter of the drops formed by ring breakup, and the ring diameter, should be a constant, as follows (Dombrowski and Hooper, 1962):

$$d_{rd}/d_r = 1.88, \quad \text{predicted.} \tag{11}$$

The Rayleigh breakup condition of (11) was evaluated using the present measurements. In doing this, the complication of the node drops was ignored (they will be considered later) and only drops formed from the intervening constant-diameter portions of the ring were considered. In addition, d_r was determined for this expression at the time of ring drop breakup, i.e. $t/t^* = 5$ where $d_r/d_o = 0.13$ from Fig. 4 with a 16% uncertainty.

The values of d_{rd}/d_r measured during the present investigation are summarized as a function of Oh in Table 2. As before, the present experiments involved a nearly constant Oh (and Oh_r) for each liquid because the variation of We is small in the bag breakup regime. The measurements do not suggest a significant effect of Oh over the present test range and yield

$$d_{rd}/d_r = 2.2, \quad \text{measured.} \tag{12}$$

Clearly, (12) is in reasonably good agreement with the Rayleigh breakup prediction at small Oh given by (11), supporting Rayleigh breakup as the mechanism producing drops from the ring-like portions of the basal ring, Finally, given $d_r/d_o = 0.13$, as just discussed, implies:

$$d_{rd}/d_o = 0.29. \tag{13}$$

The effect of the node drops on the mean size of drops produced by the ring will be considered next. In general, there were 4–6 node drops, having diameters of $(1.3–1.6)d_{rd}$. Thus, if this contribution is added to that of the drops from the tubular portions of the ring, the final average size of drops formed from the basal ring, d_{trd}, can be correlated as follows:

$$d_{trd}/d_o = 0.30 \tag{14}$$

with the uncertainty of this constant being less than 20%. Finally, the total number of drops produced by the basal ring, N_{trd}, can be found from the mean size of the basal ring drops given by (14) and the volume of the basal ring given by (8), as follows:

$$N_{trd} = 22.1.$$

3.2.4. Basal ring breakup time

As discussed by McCarthy and Molloy (1974), the Rayleigh breakup times, t_{rt} of liquid columns have been shown to be

$$t_{rt} = C(\rho_t d_r/\sigma)^{1/2}(1 + 3Oh_r)d_r \tag{16}$$

where d_r is the column diameter, Oh_r is the Ohnesorge number based on this dimension, and C is a stability constant that must be determined. Smith and Moss (1917) found C to be 13 for different liquids and column diameters. Associating the time required for the Rayleigh breakup with the time required for the basal ring to breakup, by replacing the column diameter with the tube axis diameter in (16), yields:

$$t_{rt} = CC_{rt}(\rho_L d_r/\sigma)^{1/2}(1 + 3Oh_r)d_r \tag{17}$$

where C_{rt} is an unknown constant of proportionality expected to be on the order of unity. For the conditions of the present study, Oh_r is small so that the effect of liquid viscosity represented by the Oh term can be neglected. Then, normalizing (17) by t^* yields:

$$t_{rt}/t^* = 13C_{rt}We^{1/2}(d_r/d_o)^{1/2}. \tag{18}$$

For bag breakup, $We = 13$–25. while $d_r/d_o = 0.17$–0.19 in the region where the basal ring is present (i.e. $2 \leqslant t/t^* \leqslant 5$) as seen in Fig. 4. Substituting averages of these parameters into (18) then yields:

$$t_{rt}/t^* = 3.88C_{rt}. \tag{19}$$

Finally, it is assumed that the Rayleigh breakup process of the basal ring begins when the ring has just formed ($t/t^* \approx 2$) and ends upon ring breakup ($t/t^* \approx 5$), based on the results illustrated in Fig. 1. This implies that the time required from initial basal ring formation to basal ring breakup is $t_{rt} = 3t^*$, so that $C_{rt} = 0.77$. Since C_{rt} is on the order of unity, as expected, this finding provides good support for the idea that basal ring breakup involves a relatively passive Rayleigh breakup process. Thus, given that the time required to reach maximum deformation, where basal ring formation is completed, is $2t^*$, the Rayleigh breakup time of the basal ring of roughly $3t^*$ fixes the entire bag breakup time to be roughly $5t^*$. This breakup time is nearly the same as for shear breakup (Liang et al., 1988) but the previous reasoning suggests that this agreement is fortuitous due to the very different breakup phenomena that comprise the bag and shear breakup processes.

3.2.5. Ring drop velocity distributions

Ring drop velocity distributions were essentially independent of drop size, except for a slight tendency for node drops to move slower than the smaller ring drops formed from portions of the basal ring between the node drops. This effect is evident from the downstream deflection of the basal ring in the region between nodes seen in the inset figure at $t/t^* = 4$ in Fig. 1. This variation, however, is less than present experimental uncertainties for velocity measurements so that initial ring drop velocities can be computed from the results illustrated in Fig. 2 with little error.

3.3. Bag properties

3.3.1. Bag drop diameters

The properties of drops formed by breakup of the bag, along with a few determinations of bag thickness, h, by measurements from holograms, are summarized in Table 3. It should be noted that the values of h given in Table 3 are not very reliable because they approach present limits of spatial resolution and involve additional problems of estimating film thicknesses from the region where the bag breaks up into drops (in particular, later considerations will show that unbalanced surface tension forces in the region where bag drops are forming are important so that these effects probably locally increase bag thicknesses as well). In view of these problems, it is estimated that the values of h in Table 3 might be too large by as much as a factor of two, although the corresponding drop diameter measurements for drops found from bag breakup are felt to be reliable within the uncertainties stated earlier. Entries provided in Table 3 include d_o, the time when drop sizes were measured (except for one condition at $t/t^* = 3$, these results were averaged over the entire breakup period of $t/t^* = 3$–4), the number-averaged bag drop diameter, d_{bda}, and the Sauter mean diameter, SMD_{bd}, of drops formed from the breakup of the bag, several normalizations of these properties and the Ohnesorge number based on the dimension d_{bda}.

Comparing mean drop diameters at the start of bag breakup and averaged over the entire bag breakup period for glycerol (42%) indicates an increase of the drop sizes as the basal ring of the bag is approached. This is not unexpected as some stretch of the bag membrane, and a corresponding reduction of the size of drops formed by breakup of the membrane, is expected as the farthest downstream location is approached. Nevertheless, the variation of drop diameters is not large, with drops formed initially from the bag being only 15% smaller than the mean size of drops formed from the bag.

A second issue of interest about drops formed by breakup of the bag itself is the variation of mean drop sizes with Oh. The results of Table 3 show that both d_{bda}/d_o and SMD_{bd}/d_o increase as Oh increases over the test range. Characterizing this behavior by the Ohnesorge number based on the average size of drops formed from the bag, it is seen that d_{bda}/d_o

Table 3
Summary of properties of drops formed from the bag†

Liquid‡	d_o (μm)	t/t^* (–)	h (μm)	d_{bda} (μm)	SMD_{bd} (μm)	Oh_{bda}	h/d_o (%)	d_{bda}/h (–)	d_{bda}/d_o (%)	SMD_{bd}/d_o (%)
Water	620	3–4	16.4	21.9	23.8	0.023	2.65	1.33	3.5	3.8
Glycerol (21%)	650	3–4	—	22.1	23.9	0.077	—	—	3.8	3.5
Glycerol (42%)	650	3	23.2	25.8	28.9	0.038	3.57	1.12	4.0	4.5
Glycerol (42%)	650	3–4	—	29.6	33.2	0.075	—	—	4.6	5.1
Glycerol (63%)	850	3–4	35.4	42.1	48.8	0.193	4.16	1.17	4.9	5.2
					averages =		3.46	1.21	4.2	4.4

†Results based on the properties of the bag and the properties of drops formed by breakup of the bag during the bag breakup period for the test conditions summarized in Table 1.

‡Glycerol compositions given in parentheses are percent glycerin (by mass) in water.

increases from 3.5* to 4.9* as Oh_{bda} increases from 0.023 to 0.193. This behavior suggests an effect of liquid viscosity on bag properties, and thus on the properties of drops formed from the bag; such behavior is not surprising in view of past observations (Hsiang and Faeth, 1992, 1993, 1995) of strong effects of liquid viscosity on the drop sizes formed by secondary breakup.

Mean drop sizes resulting from breakup of the bag vary somewhat with initial Oh as just noted, but yield an average value of d_{bda}/d_o of 4.2%, over the present test range. Thus, bag drops generally are relatively small and do not have as strong an effect on spray transport properties as the drops produced by breakup of the basal ring. For example, based on the diameter-squared behavior that tends to dominate drop properties in sprays (Faeth 1997), the lifetime of drops formed from the basal ring would be nearly 60 times longer than the lifetime of drops formed from the bag. Another issue concerning mean drop sizes is that SMD_{bd} and d_{bda} are nearly the same, e.g. the average value of the ratio $SMD_{bd}/d_{bda} = 0.89$. This behavior implies a nearly monodisperse size distribution for these drops, a property that will be considered in more detail next. To summarize, the correlation of bag drop sizes becomes:

$$d_{bda}/d_o = 0.042. \tag{20}$$

The size distribution function of drops formed by breakup of the bag is illustrated in Fig. 5. These results are plotted according to the root normal distribution function that has proven to

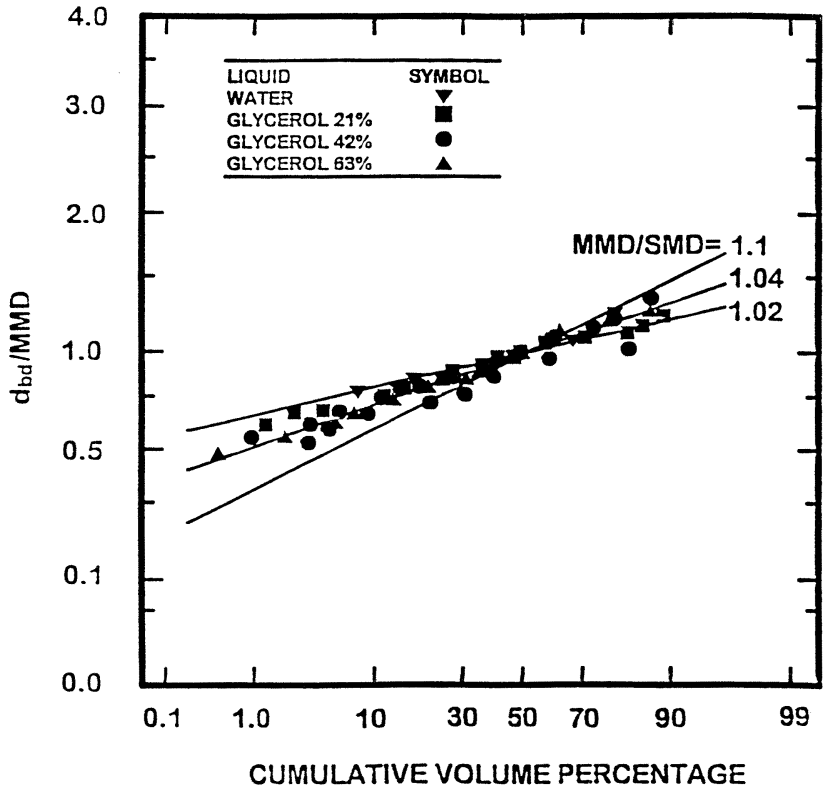

Fig. 5. Drop size distributions of drops formed from breakup of the bag itself during bag breakup.

be successful for a variety of drop and spray breakup processes (Faeth, 1997). Results for various values of MMD/SMD for the bag drops are shown on the plot for comparison with the measurements. In the past, this distribution function with $MMD/SMD = 1.20$ has been successful for correlating drop size distributions in sprays. The bag drops themselves, however, while correlating reasonably well according to the root normal distribution function, do so only with a much smaller value of $MMD/SMD = 1.04$. As discussed earlier, however, this result is not unexpected due to the nearly monodisperse size distribution of drops formed from the bag because the bag membrane itself appears to have a relatively uniform thickness. The behavior of the drop size distribution function changes when drops formed from both the bag and the ring are considered, however, as discussed later in connection with overall breakup properties.

3.3.2. Bag breakup time

The time required for breakup of the bag, t_b, is also an important parameter that must be known. This issue will be considered in the following, assuming a constant bag thickness during bag growth period with an average bag velocity, u_b as shown in Table 4, by relating the bag breakup time to the breakup time of a thin film.

From Dombrowski and Hooper (1962), the time required from breakup of a thin film, t_{ft}, can be correlated as follows:

$$t_{ft}/t^* = 3.73We^{-1/2}(u_o/u_L)^2(h/d_o)^{1/2} \tag{21}$$

where u_L is the liquid film velocity. For the bag growth period, the liquid film velocity can be approximated by u_b to yield the time required for breakup of bag as follows:

$$t_{bt}/t^* = 3.73C_{bt}We^{-1/2}(u_o/u_b)^2(h/d_o)^{1/2} \tag{22}$$

where C_{bt} is a constant of proportionality expected to be on the order of unity. Applying (22), using a constant value of $h/d_o = 1\%$, yields the bag breakup times summarized in Table 4. From Fig. 1, the time required for breakup of the bag is typically $t_{bt}/t^* = 1.0$, thus, averaging the results in Table 4 implies that the $C_{bt} = 0.91$ which is on the order of unity, as expected. This finding strongly supports the idea that breakup of the bag itself involves a simple thin film breakup of the membrane-like bag, and that the bag inflation time is controlled by the breakup time of the first part of the bag that is formed, i.e. the tip of the bag.

Table 4
Summary of properties of bag during bag formation period†

Liquid‡	We	t/t^*	h/d_o	u_b/u_o	t_{bt}/t^*
Water	15	2.0–3.5	0.01	0.266	1.36
Glycerol (21%)	15	3.0–3.5	0.01	0.288	1.16
Glycerol (42%)	17	3.0–3.5	0.01	0.324	0.92
Glycerol (63%)	15	3.0–3.5	0.01	0.317	0.96

†Result based on the properties of the bag during the bag breakup period for the test conditions summarized in Table 1.

‡Glycerol compositions given in parentheses are percent glycerin (by mass) in water.

3.3.3. Bag drop velocity distribution

Initial velocities of bag drops exhibit negligible variation with size over the narrow range of sizes of these drops. In addition, even though portions of the bag move at somewhat different velocities than the parent drop (which is taken to be the basal ring for $2 \leqslant t/t^* \leqslant 5$ when parent drop velocities are found) these velocity variations are small compared to the parent drop velocity. Thus, within present experimental uncertainties, initial bag drop velocities can be estimated as the parent drop velocity at the time they are formed from Fig. 2. Present observations indicate that the time of breakup of the bag extends over the range $t/t^* = 3.2$–3.5, thus, in view of the relatively slow variation of parent drop velocities seen in Fig. 2, initial bag drop velocities are essentially monodisperse within present experimental uncertainties.

3.4. Overall breakup properties

3.4.1. Drop size distributions

Past work yielded different observations about overall drop size distributions resulting from bag breakup, for example, Hsiang and Faeth (1992, 1993, 1995) find that drop size distribution functions were represented reasonably well by the universal root normal size distribution function while Gel'fand et al. (1974) report a bimodal drop size distribution function with one nearly monodisperse group associated with drops formed from the ring and a second nearly monodisperse group associated with drops formed from the bag. The overall drop size distribution function properties were studied during the present investigation in order to help resolve these differences. As a practical matter it was found that in spite of the nearly monodisperse drops formed from the bag, no bimodal behavior for the drop size distribution function was evident. Thus, present results concerning the drop size distribution function were correlated in terms of the universal root normal distribution function of Simmons (1977). It will be shown later, however, that this behavior probably is due to undersampling the small drops formed from the bag, tending to support the findings of Gel' fand et al. (1974) at least to the extent that an overall drop size distribution is useful for treating bag breakup processes.

The drop size distribution results for the present measurements of bag breakup properties are plotted in terms of the universal root normal distribution function in Fig. 6. These results emphasize behavior over the entire test range rather than more statistically significant results at a fewer number of conditions. Thus, the measurements illustrated in Fig. 6 are scattered due to inadequate statistics. In particular, bag breakup of individual drops yields a relatively small number of large drops that dominate the size distribution function because they represent a large fraction of the drop volume produced by breakup. In addition, the small drops formed from breakup of the bag itself tend to be undersampled because they are small and poorly resolved and also are rapidly swept downstream due to their rapid acceleration to gas velocities. The results shown in Fig. 6 however, are reasonably represented by the root normal distribution function, with $MMD/SMD = 1.2$, which is similar to earlier findings for other spray breakup processes (Faeth, 1997).

A second issue of interest about the drop size distribution is the SMD after bag breakup. The SMD is mainly dominated by the largest drop sizes in the distribution; thus, by neglecting the small drops from the bag, the present measurements of SMD/d_o after bag breakup are summarized in Table 5, along with the average ring drop size from (14) and the average bag drop size from Table 3. Clearly, the SMD after bag breakup is dominated by the node drop

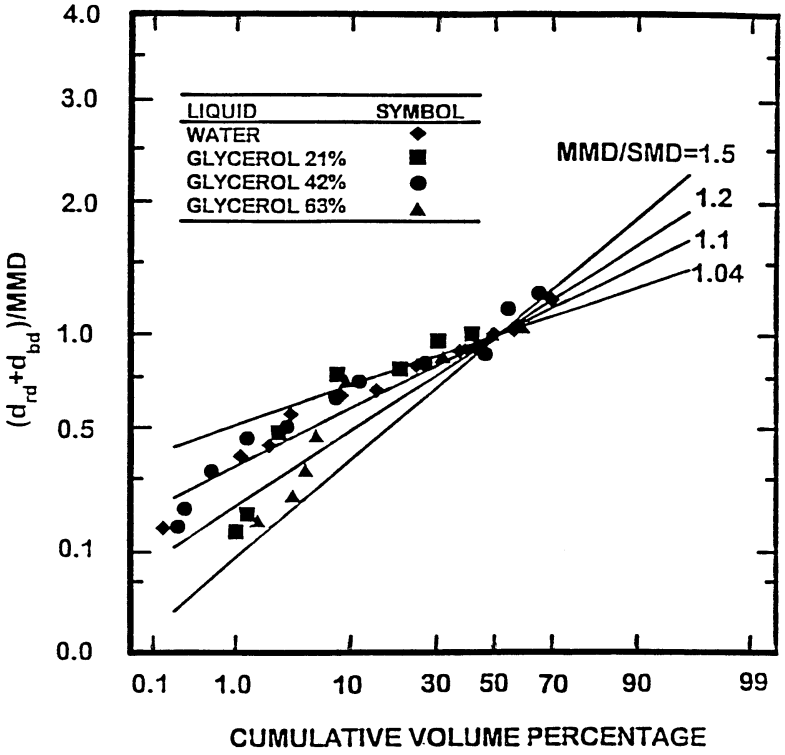

Fig. 6. Drop size distributions of drops formed from both the bag and the basal ring during the entire bag breakup process.

size (the largest drop size of ring drops) and is essentially independent of *Oh* over the present range to yield:

$$SMD_{\text{total}}/d_{\text{o}} = 0.36 \tag{23}$$

with a standard deviation of 0.05 for (23).

Table 5
Summary of *SMD* after bag breakup†

Liquid‡	*We*	*Oh*	$SMD_{\text{total}}/d_{\text{o}}$	$d_{\text{trd}}/d_{\text{o}}$	$d_{\text{bd}}/d_{\text{o}}$
Water	15	0.0043	0.34	0.30	0.035
Ethyl alcohol	15	0.015	0.32	0.30	—
Glycerol (21%)	15	0.0075	0.41	0.30	0.038
Glycerol (42%)	17	0.016	0.37	0.30	0.040
Glycerol (63%)	15	0.042	0.38	0.30	0.041
		averages =	0.36	0.30	0.041

†Result based on the properties of the bag during the bag breakup period for the test conditions summarized in Table 1.

‡Glycerol compositions given in parentheses are percent glycerin (by mass) in water.

The present correlation of the *SMD* for the entire bag breakup process from (23) differs from the earlier findings of Hsiang and Faeth (1992). The correlating expression for the *SMD* for bag breakup from Hsiang and Faeth (1992) was found as an empirical extension of the boundary layer stripping analysis developed for the shear breakup regime to yield the following expression:

$$\rho SMD u_o^2/\sigma = 6.2(\rho_L/\rho_G)^{1/4}(\nu_L/d_o u_o)^{1/2} We. \tag{24}$$

The SMD after bag breakup for the present measurements is plotted in Fig. 7 as suggested by (24), along with the data of Hsiang and Faeth (1992) for the bag breakup region. Both sets of measurements roughly agree with each other, however, the results of the present study, characterized by the results of (23), yield a constant value of SMD/d_o for the bag region instead of the correlation of (24). This implies that the *SMD* after bag breakup only fortuitously agreed with the boundary layer analogy, over the narrow range of *We* of the bag breakup regime. Thus, a more rational approach would be to treat bag breakup as dominated by Rayleigh breakup of the basal ring, including the complications due to the presence of node drops to yield (23).

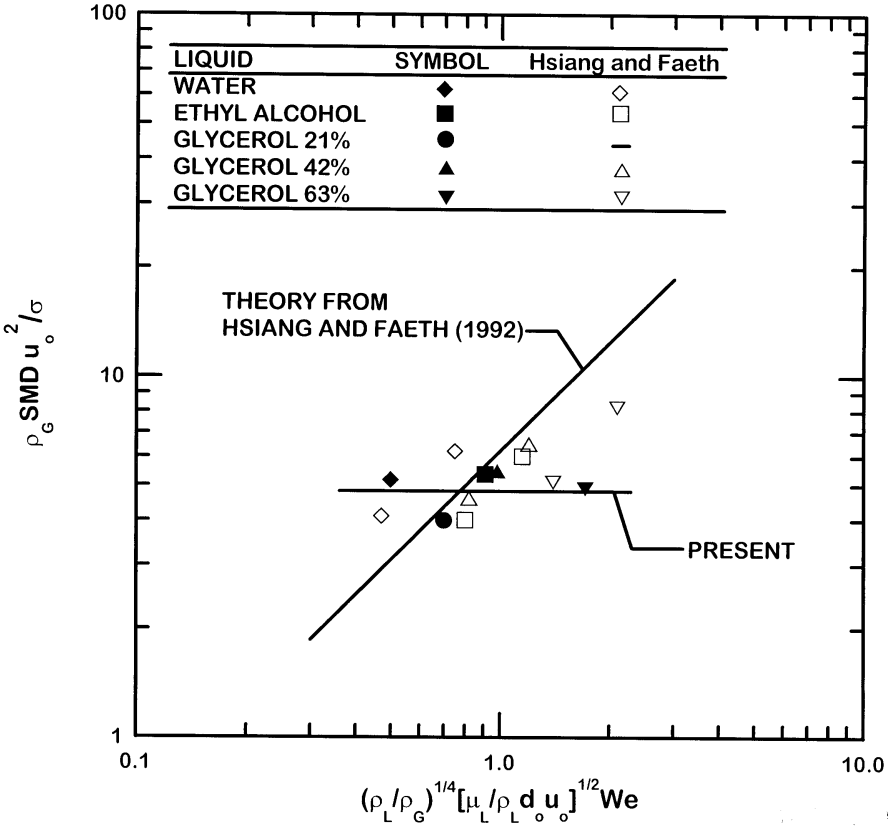

Fig. 7. Correlation of the *SMD* after the entire bag breakup process.

The small drops (which mainly are formed from the bag) can have a large effect on the *SMD*, however, even though they are often ignored, because there are a large number of small drops due to the reasonably large mass fraction and small size of drops formed from the bag. In the same way that the number of drops formed from the ring was estimated in (15), the number of drops formed from the bag can be estimated as follows:

$$\pi/6d_{\mathrm{o}}^{3}(\text{mass fraction of bag drops}) = N_{\mathrm{b}}\pi/6d_{\mathrm{bd}}^{3}. \tag{25}$$

Using the mass fraction of the basal ring from (8) and the average bag drop size given by (20), the number of drops formed from the bag can be computed from (25) to yield $N_{\mathrm{b}} = 5940$ bag drops per initial drop. Summarizing the results from (8) and (25), and estimating the number of node drops as 6 per initial drop, then the number distribution involves fixed fractions for the bag, node and ring drops as follows: $f_{\mathrm{b}} = 0.996$, $f_{\mathrm{n}} = 0.001$ and $f_{\mathrm{r}} = 0.003$. It is obvious, that the small drops dominate the number of drops in the distribution.

Given this information, the overall *SMD* including the small drops can be estimated from the fundamental definition of the *SMD* as follows:

$$SMD/d_{\mathrm{o}} = \frac{f_{\mathrm{b}}(d_{\mathrm{bd}}/d_{\mathrm{o}})^{3} + f_{\mathrm{r}}(d_{\mathrm{rd}}/d_{\mathrm{o}})^{3} + f_{\mathrm{n}}(d_{\mathrm{nd}}/d_{\mathrm{o}})^{3}}{f_{\mathrm{b}}(d_{\mathrm{bd}}/d_{\mathrm{o}})^{2} + f_{\mathrm{r}}(d_{\mathrm{rd}}/d_{\mathrm{o}})^{2} + f_{\mathrm{n}}(d_{\mathrm{nd}}/d_{\mathrm{o}})^{2}}. \tag{26}$$

Substituting the values of f_{b}, f_{r} and f_{n}, and the ratios $d_{\mathrm{bd}}/d_{\mathrm{o}}$, $d_{\mathrm{rd}}/d_{\mathrm{o}}$. $d_{\mathrm{nd}}/d_{\mathrm{o}}$, found earlier, yields $SMD/d_{\mathrm{o}} = 0.11$, which is much smaller than the result given by (23) where the bag drops have been ignored. This implies that the small drops do affect the *SMD* substantially when the overall *SMD* is sought. This behavior suggests that such gross averages for the entire bag breakup process are not very helpful, although the drops formed from the bag are still important in spite of their small size because they amount to 44* of the initial mass of the drop. Taken together, a more effective approach is to use (23) to estimate the size of the ring drops, and (20) to estimate the size of the bag drops, while treating these drops as separate populations.

3.4.2. Drop breakup rate

In order to find drop breakup rates, the fact that the entire bag breakup process involves two separate periods of liquid removal from the parent drop must be considered: one period associated with breakup of the bag itself, and the other period associated with breakup of the basal ring. The first period involves 44% of the original drop mass from (8), with this process approximated by a constant rate of liquid removal over the time period, $t/t^{*} = 3.2$–3.5, when the bag itself was observed to break up based on present measurements. The second period involves 56% of the original drop mass from (8), with this process assumed to occur by the nearly simultaneous formation of drops from the basal ring at $t/t^{*} = 5.0$, when the basal ring was observed to break up based on present measurements.

Present measurements of the cumulative volume percentage of liquid removed from the parent drop, based on the assumptions just discussed, are plotted in Fig. 8. Thus, unlike shear breakup, bag breakup involves two relatively short breakup periods, separated by periods of development of the Rayleigh breakup processes. An interesting feature of the results illustrated in Figs. 1 and 8 is that the bag forms for a time period 1.0 t^{*} with bag formation ending due

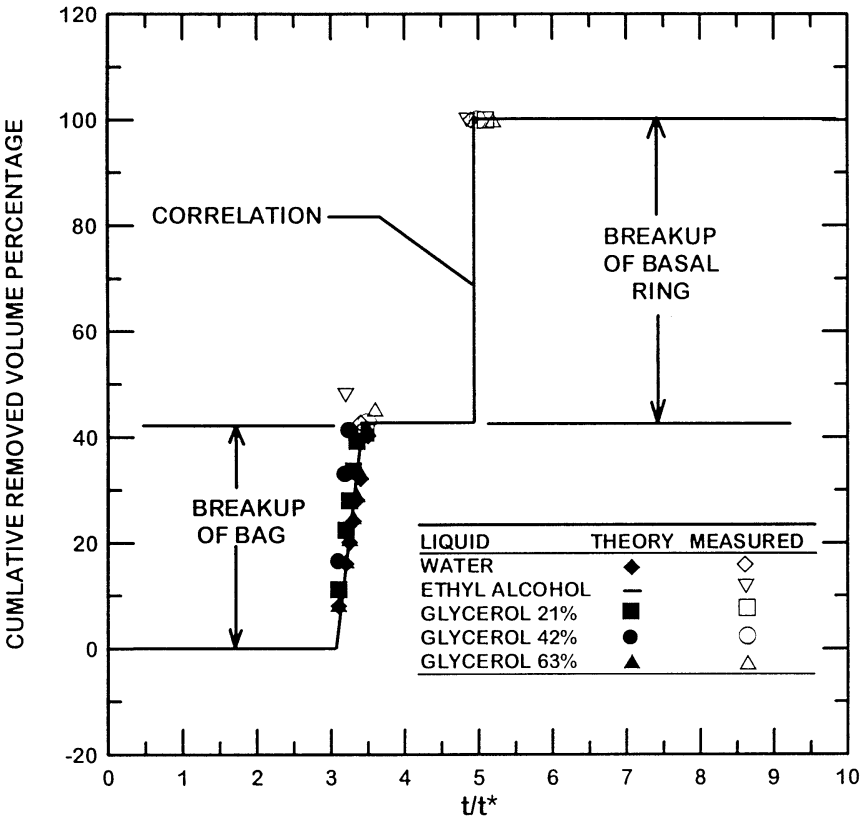

Fig. 8. Cumulative removed volume percentage of liquid from the parent drop as a function of time during bag breakup.

to Rayleigh breakup of the tip of the bag. Thus, if the entire process of breakup of the bag proceeded by passive Rayleigh breakup, a total breakup period of the bag 1.0 t^* might be expected as well. Instead, the bag actually breaks up in a much shorter time, 0.3 t^*. This suggests that once breakup of the bag starts, the unbalanced surface tension forces on the broken bag enhance its motion toward the basal ring so that its time of breakup (or disappearance) is reduced. This behavior also helps to explain the tendency for bag drop sizes to be larger than suggested by estimates of bag thickness, and to increase as the basal ring is approached due to a corresponding increase of the membrane thickness. Finally, the liquid removal properties of bag breakup highlights why separate treatment of drops formed from the bag and from the basal ring is preferable to attempting to treat all the drops as a single population.

3.4.3. Temporal and spatial breakup region

The spatial and temporal properties of bag breakup based on the velocity results of Fig. 2 are illustrated in Fig. 9. These findings involve the streamwise positions of the drops and the tip of the bag, denoted by x, as functions of the time after the start of breakup. The positions of the parent drop (which is the slowest drop to relax toward gas velocities), the tip of the bag

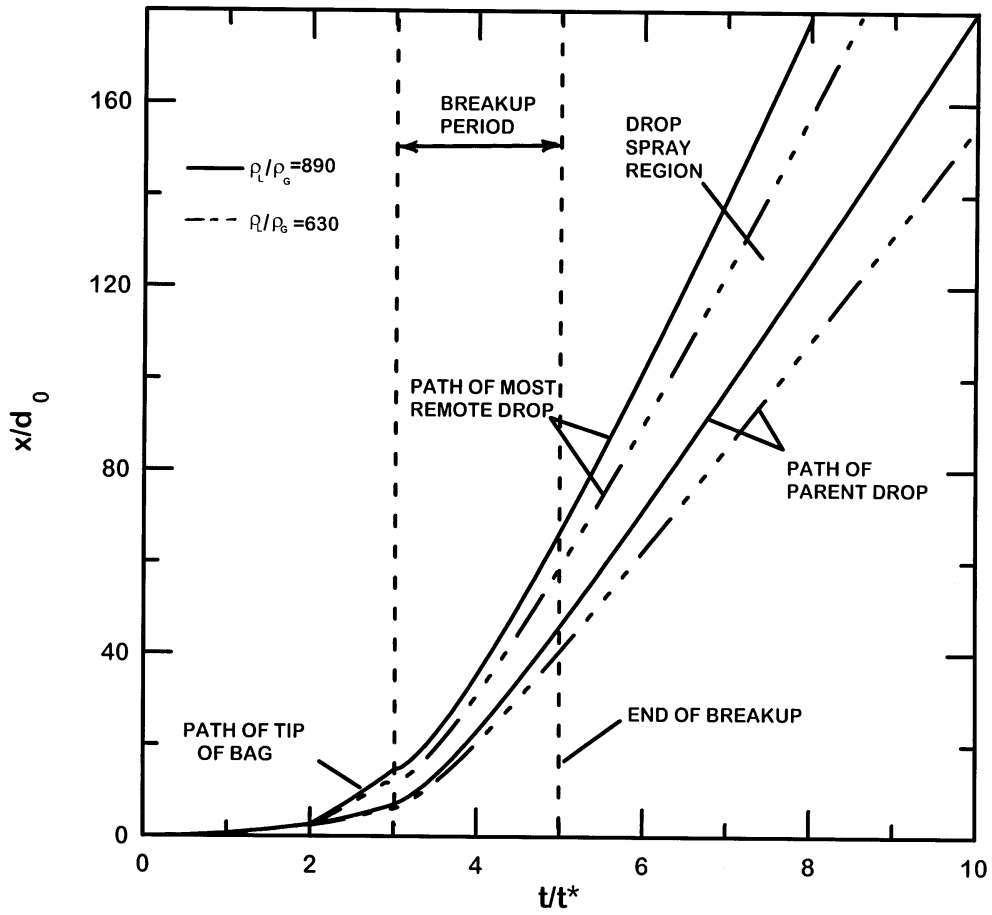

Fig. 9. Streamwise positions of the parent and the most remote drops as a function of time during bag breakup.

(when it is present in the period $2 < t/t^* < 3$) and the most remote drop (which is the first drop formed from breakup of the tip of the bag and which responds relatively rapidly to the gas motion due to its relatively small size) are illustrated in the figure. The most remote drop separates from the parent drop at roughly $t/t^* = 3$ (actually $t/t^* = 3.2$) when the bag begins to break up, and begins its streamwise travel from the tip of the bag. The breakup process itself typically is ended when breakup of the ring is completed, which occurs roughly at $t/t^* = 5$ for present test conditions. In the coordinate system of Fig. 9, there is a small effect of ρ_L/ρ_G on drop motion; therefore, results at the limits of the present test range, $\rho_L/\rho_G = 630$ and 890, have been illustrated on the plot.

The results illustrated in Fig. 9 indicate that the temporal and spatial ranges of bag breakup are comparable to the findings for shear breakup observed by Chou et al. (1997). In particular, the breakup period requires t/t^* in the range 0–5; in this period, the most remote drop moves a streamwise distance of roughly 60 initial drop diameters and the parent drop moves a streamwise distance of roughly 50 initial drop diameters. Finally, the results plotted in Fig. 1 (based on the value of d_p/d_o at the time of breakup of the basal ring) imply that the largest

drops formed by breakup of the ring spread laterally to a diameter of roughly 7 initial drop diameters. These times and distances are comparable to characteristic times and distances associated with the dense region of pressure-atomized sprays (Faeth, 1997); therefore, both bag and shear breakup should be treated as rate processes rather than by jump conditions, in many instances.

4. Conclusions

The objective of the present study was to experimentally investigate the temporal properties of bag breakup for shock-wave initiated disturbances in air at normal temperature and pressure. The test liquids included water, ethyl alcohol and various glycerol mixtures to yield liquid/gas density ratios of 633–893, Weber numbers of 13–20, Ohnesorge numbers of 0.0043–0.0427 and Reynolds numbers of 1550–2150. The major conclusions of the study are as follows:

1. The basal ring formed from the parent drop contains roughly 56% of the initial drop volume (mass) and eventually yields drops having mean diameters of roughly 30% of the initial drop diameter due to a Rayleigh-like breakup process of the basal ring that occurs relatively abruptly near $t/t^* = 5$.
2. The bag formed from the parent drop contains roughly 44% of the initial drop volume (mass) and eventually yields nearly monodisperse drops having mean diameters of roughly 4% of the initial drop diameter due to a breakup process of the membrane-like bag. This breakup process propagates progressively from the tip to the basal ring end of the bag over the period $t/t^* = 3.2$–3.5 and yields a nearly monodisperse drop size distribution; this behavior suggests a relatively uniform bag thickness of roughly 2–3% of the initial drop diameter.
3. The distinct properties of the drops formed from the bag and from the basal ring suggest that they should be treated as separate drop populations rather than merged as in past determinations of bag breakup jump conditions, e.g. the approach developed by Hsiang and Faeth (1992). Thus, the two drop populations should be represented by separate size distribution functions with the bag drops assumed to be formed at a uniform rate over the period $t/t^* = 3.2$–3.5 and the basal ring drops assumed to be formed abruptly at $t/t^* = 5.0$, with initial drop velocities at these conditions relatively independent of drop size and approximated by corresponding parent drop velocities at the time of drop formation.
4. The parent drop experiences large acceleration rates due to the development of both large cross-sectional areas and large drag coefficients caused by drop deformation and bag formation. Phenomenological analyses provided reasonably good correlations of parent drop velocities similar to earlier considerations of jump conditions for drop velocities due to Hsiang and Faeth (1992, 1993, 1995).
5. Bag breakup causes significant temporal and spatial dispersion of drops during the breakup period, as follows: the breakup process requires a total time of $t/t^* = 5$; the cross-stream dispersion, based on the diameter of the ring axis when ring breakup is completed, amounts to roughly 7 initial drop diameters; and the streamwise dispersion when breakup is

completed involves a streamwise motion of the parent drop of roughly 50 initial drop diameters and corresponding motion of the most remote drop of roughly 60 initial diameters. These times and distances are not always small in comparison to the characteristic times and distances of dense spray processes, implying that bag breakup should be treated as a rate process, rather than by jump conditions, in some instances, in agreement with earlier findings for shear breakup due to Chou et al. (1997).

Acknowledgements

This research was sponsored by the Air Force Office of Scientific Research, grant no. F49620-95-1-0364, under the technical management of J.M. Tishkoff, and the Office of Naval Research under the technical management of E.P. Rood. The authors would like to thank C.W. Kauffman for the loan of the shock tube facility and advice concerning its operation. The U.S. Government is authorized to reproduce and distribute copies of this article for governmental purposes notwithstanding any copyright notation thereon.

References

Chou, W-H., 1997. Temporal variation of drop properties and formation rates during secondary breakup. Ph.D. thesis, The University of Michigan, Ann Arbor, Michigan, U.S.A.

Chou, W.H., Hsiang, L-P., Faeth, G.M. 1997. Temporal properties of secondary drop breakup in the shear breakup regime. Int. J. Multiphase Flow, 23, 651–669.

Dombrowski, H., Hooper, P.C., 1962. The effect of ambient density on drop formation in sprays. Chem. Engr. Sci. 19, 291–305.

Faeth, G.M. 1997. Spray combustion phenomena. In: Twenty-Sixth Symposium (International) on Combustion. The Combustion Institute, Pittsburgh, Pennsylvania, U.S.A., pp. 1593–1612.

Faeth, G.M., Hsiang, L-P., Wu, P-K., 1995. Structure and breakup properties of sprays. Int. J. Multiphase Flow 21 (Suppl.), 99–127.

Gel'fand, B.E., Gubin, S.A., Kogarko, S.M., 1974. Various forms of drop fractionation in shock waves and their special characteristics. Inzhenerno-Fizicheskii Zhurnal 27, 119–126.

Hsiang, L-P., Faeth, G.M., 1992. Near-limit drop deformation and secondary breakup. Int. J. Multiphase Flow 18, 635–652.

Hsiang, L-P., Faeth, G.M., 1993. Drop properties after secondary breakup. Int. J. Multiphase Flow 19, 721–735.

Hsiang, L-P., Faeth, G.M., 1995. Drop deformation and breakup due to shock wave and steady disturbances. Int. J. Multiphase Flow 21, 545–560.

Lane, W.R., 1951. Shatter of drops in streams of air. Ind. Engr. Chem. 43, 1312–1317.

Lange, N.A., 1952. Handbook of Chemistry, 8th ed. Handbook Publishers, Sandusky, Ohio, p. 1134 and 1709.

Liang, P.Y., Eastes, T.W., Gharakhari, A., 1988. Computer simulations of drop deformation and drop breakup. AIAA Paper No. 88-3142.

McCarthy, M.J., Malloy, N.A., 1974. Review of stability of liquid jets and the influence of nozzle design. Chem, Engr. J. 7, 1–20.

Ranger, A.A., Nicholls, J.A., 1969. The aerodynamic shattering of liquid drops. AIAA J. 7, 285–290.

Simmons, H.C., 1977. The correlation of drop-size distributions in fuel nozzle sprays. J. Engr. Power 99, 309–319.

Smith, S.W.J., Moss, H., 1917. Mercury jets. Proc. Roy. Soc. 93, 373–393.

White, F.M., 1974. Viscous Fluid Flow. McGraw–Hill, New York.

Wu, P-K., Ruff, G.A., Faeth, G.M., 1991. Primary breakup in liquid/gas mixing layers for turbulent liquids. Atomization and Sprays 1, 421–440.

Wu, P-K., Hsiang, L-P., Faeth, G.M., 1995. Aerodynamic effects on primary and secondary breakup. Prog. Astro. Aero. 169, 247–279.